



## Measurement of $t\bar{t}$ Production Cross Section in the Lepton + Tau + b-jet(s) + $\cancel{E}_T$ Channel Using $1.2 \text{ fb}^{-1}$ of Run IIb Data

The D0 Collaboration  
URL: <http://www-d0.fnal.gov>  
(Dated: July 9, 2008)

We describe a measurement of the production cross section of top quark pairs in the lepton+tau channel using  $1.2 \text{ fb}^{-1}$  of data, collected by the D0 detector at the Fermilab Tevatron  $p\bar{p}$  collider during Run IIb. We select events with one isolated high  $p_T$  electron or muon, one isolated hadronic tau candidate, missing transverse energy, and two or more high  $p_T$  jets. The signal-to-background ratio is improved by applying a neural network  $b$ -tagging algorithm. We select 19 candidate events in the  $\mu + \tau$  channel, and 17 candidate events in the  $e + \tau$  channel. We measure the top pair production cross section (assuming standard model decay branching ratios and a top mass of 170 GeV) to be:

$$\begin{aligned}\mu + \tau : \sigma(t\bar{t}) &= 7.84_{-2.28}^{+2.66}(\text{stat})_{-1.44}^{+1.46}(\text{syst}) \pm 0.48(\text{lumi}) \text{ pb}, \\ e + \tau : \sigma(t\bar{t}) &= 5.05_{-2.51}^{+2.95}(\text{stat})_{-2.23}^{+2.25}(\text{syst}) \pm 0.31(\text{lumi}) \text{ pb}.\end{aligned}$$

The combination of the both  $e\tau$  and  $\mu\tau$  channels gives:

$$\ell + \tau : \sigma(t\bar{t}) = 6.75_{-1.70}^{+1.91}(\text{stat})_{-1.31}^{+1.49}(\text{syst}) \pm 0.39(\text{lumi}) \text{ pb}.$$

The combination of the Run IIa results and these Run IIb results gives (assuming a top mass of 175 GeV):

$$\ell + \tau : \sigma(t\bar{t}) = 7.32_{-1.24}^{+1.34}(\text{stat})_{-1.06}^{+1.20}(\text{syst}) \pm 0.45(\text{lumi}) \text{ pb}.$$

## I. INTRODUCTION

The Fermilab Tevatron  $p\bar{p}$  collider is currently the only accelerator in the world where top quarks can be produced. Top quarks are dominantly produced in pairs ( $t\bar{t}$ ) via the strong interaction. The standard model (SM) predicts that the top quark decays always to a  $W$  boson and a  $b$  quark. The decay modes of the  $W$  boson define the possible final states. The cross section for pair production of top quarks has been measured in numerous channels for Run IIa including dileptons [1, 2], lepton+jets [3, 4], all jets [5, 6] and  $\tau$ +leptons [7] channels. This note describes the measurement of the  $t\bar{t}$  production cross section in the lepton+tau+b-jet(s)+missing transverse energy ( $\cancel{E}_T$ ) channel, where one  $W$  boson decays to a lepton (electron or muon and the corresponding neutrino) while the other decays to a  $\tau$  and a  $\nu_\tau$ . Only hadronic decays of the  $\tau$  are considered.

In the following,  $e\tau$  ( $\mu\tau$ ) channel refers to  $e+\tau+b$ -jets+ $\cancel{E}_T$  ( $\mu+\tau+b$ -jets+ $\cancel{E}_T$ ) final state. The analysed Run IIb dataset was collected between July 2006 and August 2007. After data quality requirements, the total integrated luminosity available for each,  $\mu\tau$  and  $e\tau$ , channel is  $1216 \pm 74 \text{ pb}^{-1}$  [8]. This measurement will be combined with the Run IIa measurement of the  $t\bar{t}$  production cross section in the  $\tau$ +leptons channel, for a total integrated luminosity of  $2.1 \text{ fb}^{-1}$ .

## II. D0 DETECTOR

The D0 detector consists of a central tracking system, calorimeter, and outer muon system. The central tracking system surrounds the interaction region with a silicon microstrip detector (SMT) and a fiber tracker (CFT) within a 2 T solenoidal magnet. During spring 2006, an additional layer for the silicon tracker was installed close to the beam pipe, improving charged particle momentum resolution and heavy flavor identification. A preshower detector lies between the solenoidal magnet and the calorimeter for improved identification of electrons and photons. The calorimeter is composed of liquid argon calorimeter and inter-cryostat detector (ICD). The calorimeter is divided into a central region ( $|\eta_{det}| < 1.1$ ), where  $\eta_{det}$  is the pseudorapidity measured from the detector center, and a forward region ( $1.4 < |\eta_{det}| < 4.0$ ), each housed in a separate cryostat. The ICD covers the intermediate region. The outer muon system contains 3 layers of scintillators and drift tubes with a toroid magnet between the first two layers. Additional details of the detector are available in [9].

## III. EVENT RECONSTRUCTION

Electrons are reconstructed in the electromagnetic (EM) and hadronic layers (HAD) of the calorimeter by clustering energy in cells within a cone of  $\Delta R = \sqrt{(\Delta\phi)^2 + (\Delta\eta)^2} < 0.4$ . They are required to be in the central region of the calorimeter ( $|\eta| < 1.1$ ) and more than 90% of the energy must lie in the EM layers. A central track must be spatially matched to the cluster, and it must be isolated from significant energy in the hadronic calorimeter. A likelihood discriminant identifies electrons using information on the shower shape and the matched central track [1].

Muons must be reconstructed in all three layers of the muon system. We consider muons which are reconstructed with  $|\eta| < 1.8$ . They must be spatially matched to a track in the central tracking system, and are required to be isolated. Two criteria were used for muon isolation: (1) the sum of the energy deposited in the calorimeter within a hollow cone of  $0.1 < \Delta R < 0.4$  must be less than 8% of the muon energy, and (2) the sum of the  $p_T$  of tracks surrounding the muon within  $\Delta R < 0.5$  must be less than 6% of the muon  $p_T$  [1].

Jets are reconstructed from energy in the calorimeter using an iterative, seed-based cone algorithm including mid-points with a cone radius of  $R = \sqrt{(\Delta y)^2 + (\Delta\phi)^2} = 0.5$  [10]. Jet energy scale corrections are applied to bring the energy of the jets back to the particle level. For jets which contain muon with  $\Delta R(\mu, jet) < 0.5$ , the corrections include semileptonic corrections which are assumed due to the decay of heavy flavors to muons. Only muon with a  $p_T$  below 60 GeV are used to avoid arbitrarily large jet energy due to bad muon  $p_T$  resolution at high  $p_T$ . They must be reconstructed within  $|\eta| < 2.5$ .

The missing transverse energy is calculated by performing a vectorial sum of the transverse energies of all calorimeter cells surviving various noise suppression algorithms. This raw quantity is then corrected for the energy corrections applied to the reconstructed objects (electrons, taus and jets) and for the momentum of all muons in the event, corrected for their energy loss in the calorimeter.

Taus are reconstructed from energy in the calorimeter and one or more tracks. The tau cone reconstruction algorithm uses a cone size of  $\Delta R = 0.5$ . An inner cone of size  $\Delta R = 0.3$  is used to calculate tau isolation variables. We require that they are inside the central region of the calorimeter ( $|\eta| < 1.0$ ). An electromagnetic sub cluster may also be associated with the tau candidate. Tracks (ordered in decreasing  $p_T$ ) within a cone of  $\Delta R = 0.5$  may be

matched to the tau candidate as long as the mass calculated using the tracks is less than the tau mass, and no more than three tracks are already matched. The reconstructed tau candidates are classified into three categories:

1. **Type 1:** One track without any associated electromagnetic sub clusters. This type of tau candidate is expected to come from the decay  $\tau^- \rightarrow \pi^- + \nu_\tau$ .
2. **Type 2:** One track with associated electromagnetic sub cluster. This type of tau candidate is expected to come from the decay  $\tau^- \rightarrow \pi^- + n\pi^0 + \nu_\tau$ , where there are  $n \geq 1$  neutral pions.
3. **Type 3:** Two or three tracks. This type of tau candidate is expected to come from the decay  $\tau^- \rightarrow \pi^- \pi^+ \pi^- + \nu_\tau + n\pi^0$ , where there can be  $n \geq 0$  neutral pions.

The presence of a neutrino in the decay means that the visible (measured) part of the transverse momentum is substantially less than the true  $p_T$  of the tau.

Several neural networks ( $NN_\tau$ ), one for each tau type, have been trained to separate real taus from jets which fake taus. The variables used in  $NN_\tau$  are derived from tau tracks quantities, hadronic and electromagnetic calorimeter cluster energies, and shower shape. Additional description of some of the variables can be found in Ref. [11]. We require  $NN_\tau > 0.8$  for all tau types for both  $\mu\tau$  and  $e\tau$  channels. Using  $W(\rightarrow e\nu)$ +jets events, we determine a data/MC correction factor on the rate for fake taus from jets of  $0.96 \pm 0.08$ . Another neural network ( $NN_{elec}$ ) is used to separate type 2 taus from electrons. For the  $NN_{elec}$ , a subset of  $NN_\tau$  input variables are used, together with variables based on the electromagnetic cluster and the leading tau track. The  $e\tau$  analysis requires tau candidates to pass  $NN_{elec} > 0.85$ . In addition the  $e\tau$  analysis removes tau candidates with track  $\phi$  less than 0.02 radian from the nearest calorimeter module boundary, which are likely mis-reconstructed electrons.

The presence of one or more  $b$ -quark jets is a powerful discriminator between signal top quark events and background events. In this analysis we use a neural network ( $NN_b$ ) algorithm to identify if a jet originated from a  $b$ -quark [12]. We require data events to have at least one jet with  $NN_b > 0.65$  which results in an average efficiency of 54% for  $b$ -jets and an average light jet mistag rate of 1%. In Monte Carlo (MC) events, we assign a probability to each jet in the event to have originated from a  $b$ -quark. This probability is measured from data and is often referred to as the ‘‘tag rate function’’.

#### IV. SIGNAL AND BACKGROUND MODELS

Standard model backgrounds arise from electroweak  $W$  boson production and leptonic decay accompanied with jets ( $W$ +jets),  $Z/\gamma^*(\rightarrow \ell^+\ell^-)$  production accompanied with jets ( $Z/\gamma^*$ +jets), dibosons ( $WW$ ,  $WZ$  and  $ZZ$ ), single top productions and QCD multijets events when a jet fakes a tau, an electron or a muon. The  $t\bar{t}$ ,  $W$ +jets and  $Z/\gamma^*$ +jets processes are generated using ALPGEN v2.11 [13] interfaced with PYTHIA v6.409 [14]. The factorization scale chosen was  $Q^2 = M_V^2 + p_T^{j,2}$ , where  $p_T^{j,2}$  is the sum of jet  $p_T$  squared and  $V$  refers to the vector boson type ( $W$  or  $Z$ ). The diboson processes are generated using PYTHIA and single top processes using COMPHHEP generator [15]. In all samples, TAUOLA [16] is used to decay tau leptons, to handle the tau polarization properly. EVTGEN [17] is used to decay  $b$  hadrons.

Background from  $Z/\gamma^*(\rightarrow \ell\ell)$ +jets, single top and diboson processes are determined using MC, whereas contribution due to multijet production is estimated from data. Background due to  $W(\rightarrow \ell\nu)$ +jets process is determined using both data and MC, as discussed later. We have generated both  $t\bar{t} \rightarrow$  dileptons and  $t\bar{t} \rightarrow$  lepton+jets with a top mass of 170 GeV and 175 GeV. All plots and expected numbers of events given in this note are calculated for a top mass of 170 GeV.

The  $Z/\gamma^*$ +jets MC is normalized to the next-to-next-leading order (NNLO) cross section [18]. The heavy to light flavor ratio in ALPGEN  $W$ +jets and  $Z/\gamma^*$ +jets MC are corrected with factors determined from data/MC comparisons.

#### V. EVENT SELECTION

Selected events in the  $\mu\tau$  ( $e\tau$ ) channel satisfy the requirements of at least one of the the single muon (electron) or  $\mu$ +jets ( $e$ +jets) triggers. The event primary vertex is required to be within the acceptance of the SMT ( $|z_{PV}| < 60$  cm, where  $z$  is measured from the detector center along the beam direction), and to have  $\geq 3$  tracks attached. There has to be at least two jets with  $p_T > 20$  GeV and within  $|\eta_{det}| < 2.5$ , of which the leading jet has  $p_T > 30$  GeV.

For the  $\mu\tau$  channel, there has to be exactly one isolated muon with  $p_T > 20$  GeV, within  $|\eta_{det}| < 1.8$ , and coming from the vicinity of the primary vertex, ( $|\Delta z(\mu, PV)| < 1.0$  cm). No isolated electron with  $p_T > 15$  GeV

within  $|\eta_{det}| < 1.1$  is allowed in an event. In addition, a cut on the difference  $\Delta\phi$  between the azimuthal angles of the lepton momentum and the missing transverse energy vector is applied to reject events in which the transverse energy imbalance arises from the lepton energy mis-measurement. This requirement depends on the value of  $\cancel{E}_T$ :  $\Delta\phi(\mu, \cancel{E}_T) > 2.1 - 0.035\cancel{E}_T/\text{GeV}$  and  $\cancel{E}_T > 15$  GeV is also required to reject multijets events.

For the  $e\tau$  channel, there has to be exactly one isolated electron with  $p_T > 15$  GeV, within  $|\eta_{det}| < 1.1$  and coming from the vicinity of the primary vertex, ( $|\Delta z(e, \text{PV})| < 1.0$  cm). No isolated muon with  $p_T > 15$  GeV within  $|\eta_{det}| < 1.8$  is allowed in an event. A cut on the difference  $\Delta\phi$  between the azimuthal angles of the lepton momentum and the missing transverse energy vector is applied  $\Delta\phi(e, \cancel{E}_T) > 2.2 - 0.045\cancel{E}_T/\text{GeV}$  and  $\cancel{E}_T > 20$  GeV is also required to reject multijets events.

The  $W$ +jets MC is normalized to data by fitting the transverse mass distribution after only requiring an isolated muon or electron, two jets, and missing transverse energy. We subtract the estimated contributions of  $Z/\gamma^*$ +jets and  $t\bar{t}$  before performing the fit. The template for multijet events at this selection stage is obtained from data events which have a non-isolated muon or electron, two jets, and missing transverse energy. As the contribution of  $W$ +jets events passing these latter conditions has to be subtracted from the multijet template, an iterative fit is performed.

Each event is required to have one tau candidate within  $|\eta| < 1.0$ . The  $\tau$  must come from the same vertex as the lepton ( $\Delta z(\ell_t, \tau_{lt}) < 1$  cm), where  $\tau_{lt}$  is the tau's leading track and  $\ell_t$  the lepton's track, but must be separated from the lepton ( $\sqrt{\Delta\phi^2(\tau_{lt}, \ell_t) + \Delta\eta^2(\tau_{lt}, \ell_t)} > 0.5$ ). The jet multiplicity is recalculated removing any jet in the vicinity of the  $\tau$  candidate ( $\sqrt{\Delta\phi^2(\tau, \text{jet}) + \Delta\eta^2(\tau, \text{jet})} > 0.5$ ). The  $\cancel{E}_T$  is corrected for the reconstructed  $\tau$  ( $\cancel{E}_T^\tau$ ). To further reduce multijet background, we require  $\cancel{E}_T^\tau > 15$  GeV and  $\Delta\phi(\mu, \cancel{E}_T^\tau) > 2.2 - 0.045\cancel{E}_T^\tau$  in  $\mu\tau$  channel, and  $\cancel{E}_T^\tau > 20$  GeV and  $\Delta\phi(e, \cancel{E}_T^\tau) > 2.1 - 0.035\cancel{E}_T^\tau$  in  $e\tau$  channel. In the  $e\tau$  channel, a cut on the anti-electron neural network ( $NN_{elec} > 0.85$ ) is applied. The remaining events are referred to as the pre-tagged sample.

This lepton+jets+tau events sample is divided into two non-overlapping samples. The first sample contains lepton-tau pairs with opposite charge sign (OS) while the second sample contains the lepton-tau pairs which have same-sign charge (SS). Under the assumption that the multijet processes contribute equally to the SS sample and OS sample,  $N_{Multijet}^{OS} = N_{Multijet}^{SS}$ , events with SS charge lepton-tau pair are used to estimate the contribution of multijet processes in the OS sample. It is computed by subtracting the contributions of  $t\bar{t}$  and background samples to the SS data sample :

$$N_{Multijet}^{OS} = N_{Multijet}^{SS} = N_{DATA}^{SS} - N_{W+jets}^{SS} - N_{t\bar{t}}^{SS} - N_{Z/\gamma^*+jets}^{SS} - N_{diboson}^{SS} - N_{singletop}^{SS}$$

In the final selection, we require that at least one of the jets is tagged as coming from a  $b$ -quark (tagged sample). This improves the signal-to-background ratio and this sample is used for the cross section measurements. Table I lists the observed numbers of events in the SS sample for the multijet background estimation at the tagged stage. Table II lists the observed and expected numbers of events at the pre-tagged and tagged stages.

Figures 1 and 2 show distributions of the lepton  $p_T$ , the tau  $E_T$ , the leading jet  $p_T$  and the  $\cancel{E}_T^\tau$  for the  $\mu\tau+e\tau$  samples, before and after  $b$ -tagging. The agreement between expectation and the observed data is satisfactory.

## VI. CROSS SECTION EXTRACTION

As the number of events after the final selection is small, simple counting methods to extract the cross section are used. Standard model branching ratios are assumed. The contributions of various processes into the OS and SS samples can be written :

$$N_{DATA}^{OS} = N_{t\bar{t}}^{OS} + N_{W+jets}^{OS} + N_{Multijet}^{OS} + N_{Z/\gamma^*+jets}^{OS} + N_{diboson}^{OS} + N_{singletop}^{OS}$$

TABLE I: Observed same-sign events in data, and the expected amount (with statistical uncertainties) of events to be subtracted from SS data to get estimation of multijet background in the opposite sign sample, before and after  $b$ -tagging.

Sample	$\mu\tau$ channel		$e\tau$ channel	
	before $b$ -tagging	after $b$ -tagging	before $b$ -tagging	after $b$ -tagging
SS data	31.00±5.56	2.00±1.97	45.00±7.24	7.00±3.18
SS $t\bar{t} \rightarrow \ell$ +jets	4.91±0.12	2.85±0.08	7.03±0.15	4.19±0.11
SS $t\bar{t} \rightarrow \ell\ell$ +jets	0.46±0.02	0.25±0.01	0.60±0.02	0.36±0.02
SS $W$ +jets	35.24±2.82	2.45±0.17	30.09±2.48	2.06±0.14
SS diboson	1.57±0.25	0.16±0.04	1.77±0.35	0.12±0.04
SS single top	0.35±0.01	0.18±0.01	0.39±0.01	0.21±0.01
SS $Z$ +jets	4.85±0.38	0.36 ±0.02	5.17±0.40	0.32 ±0.03
Multijet	-16.38±6.25	-4.25±1.98	0.05±7.67	0.25±3.19

TABLE II: Numbers of signal and background events expected, and numbers of observed events, before and after  $b$ -tagging. Standard model cross section (7.91 pb) and branching ratios are assumed for  $t\bar{t}$  production. Uncertainties are statistical only.

	$\mu\tau$ channel		$e\tau$ channel	
	before $b$ -tagging	after $b$ -tagging	before $b$ -tagging	after $b$ -tagging
Multijet	-16.38±6.25	-4.25±1.98	0.05±7.67	0.25±3.19
$W \rightarrow \ell\nu$ (+jets)	43.07±2.75	3.39±0.23	44.86±3.92	3.08±0.17
$Z \rightarrow \mu^- \mu^+ (e^- e^+)$ (+jets)	19.69±0.73	1.52±0.05	7.51±0.51	0.47±0.03
$Z \rightarrow \tau^- \tau^+$ (+jets)	10.68±0.60	0.76±0.06	14.81±0.77	0.97±0.04
diboson	4.52±0.48	0.36±0.05	3.70±0.48	0.28±0.04
single top	0.49±0.01	0.25±0.01	0.49±0.01	0.26±0.01
$t\bar{t} \rightarrow \ell$ +jets	11.97±0.18	7.46±0.13	15.61±0.22	9.95±0.16
$t\bar{t} \rightarrow \ell\ell$ +jets non- $\mu\tau_h(e\tau_h)$	6.29±2.39	4.39±0.20	1.52±0.10	1.03±0.09
$t\bar{t} \rightarrow \mu\tau_h(e\tau_h)$ +jets	7.45±0.07	5.24±0.05	7.82±0.07	5.52±0.06
total	87.79±6.91	19.12±2.00	96.28±8.68	21.32±3.20
data		103	94	17

TABLE III: Efficiencies in % of the lepton+tau+ $b$ -jet(s)+ $\cancel{E}_T$  selection for  $t\bar{t} \rightarrow$  inclusive sample. The first row shows the efficiency for opposite-sign events taking into account the SM branching ratio, the second row is for same-sign events using the SM branching ratio. Uncertainties are statistical only.

Process	$\mu\tau$ efficiency	$e\tau$ efficiency
Opposite-sign $t\bar{t}$		
$t\bar{t} \rightarrow$ inclusive	0.1777 ± 0.0015	0.1717 ± 0.0018
Same-sign $t\bar{t}$		
$t\bar{t} \rightarrow$ inclusive	0.0322 ± 0.0008	0.0473 ± 0.0011

and

$$N_{DATA}^{SS} = N_{t\bar{t}}^{SS} + N_{W+jets}^{SS} + N_{Multijet}^{SS} + N_{Z/\gamma^*+jets}^{SS} + N_{diboson}^{SS} + N_{singletop}^{SS}$$

The contribution from multijet events to the OS and SS samples are assumed equal,  $N_{Multijet}^{OS} = N_{Multijet}^{SS}$ . The contribution from  $t\bar{t}$  processes to the OS and SS samples can be written in function of  $\sigma_{t\bar{t}}$  :  $N_{t\bar{t}}^{OS(SS)} = \varepsilon_{t\bar{t}}^{OS(SS)} \sigma_{t\bar{t}} \mathcal{L}$  where  $\varepsilon_{t\bar{t}}^{OS(SS)}$  are the efficiencies, given in table III and  $\mathcal{L}$  the integrated luminosity.  $\sigma_{t\bar{t}}$  is then solved exactly,

$$\sigma_{t\bar{t}} = \frac{N_{DATA}^{OS} - N^{bkg}}{\varepsilon \cdot \mathcal{L}}.$$

where  $\varepsilon = \varepsilon_{t\bar{t}}^{OS} - \varepsilon_{t\bar{t}}^{SS}$ .

For each individual channel  $j$ ,  $e\tau$  and  $\mu\tau$ , the observed number of events is defined by  $N_j^{obs} = N_{DATA_j}^{OS}$  and the expected number of background events is defined by

$$N_j^{bkg} = N_{DATA_j}^{SS} + (N_{W+jets_j}^{OS} - N_{W+jets_j}^{SS}) + (N_{Z/\gamma^*+jets_j}^{OS} - N_{Z/\gamma^*+jets_j}^{SS}) + (N_{diboson_j}^{OS} - N_{diboson_j}^{SS}) + (N_{singletop_j}^{OS} - N_{singletop_j}^{SS})$$

Then, the following likelihood function is estimated :

$$L(\sigma_j, \{N_j^{obs}, N_j^{bkg}, \mathcal{B}, \mathcal{L}_j, \varepsilon_j\}) = \mathcal{P}(N_j^{obs}, \mu_j) = \frac{\mu_j^{N_j^{obs}}}{N_j^{obs}!} e^{-\mu_j}$$

where  $\mathcal{P}(N_j^{obs}, \mu_j)$  is the Poisson probability to observe  $N_j^{obs}$  events given an expected combined signal and background yield of :  $\mu_j = \sigma_j \varepsilon_j \mathcal{B} \mathcal{L}_j + N_j^{bkg}$ .

Here  $\mathcal{L}_j$  is the luminosity,  $\varepsilon_j = \varepsilon_{t\bar{t}}^{OS} - \varepsilon_{t\bar{t}}^{SS}$ , the branching fraction  $\mathcal{B}$  is set to 1 since efficiencies already included it. The cross section is extracted by minimizing the negative log-likelihood function  $-\log L(\sigma_j, \{N_j^{obs}, N_j^{bkg}, \mathcal{B}, \mathcal{L}_j, \varepsilon_j\})$ .

## VII. SYSTEMATICS UNCERTAINTIES

The relative uncertainty on the luminosity is 6.1%. The corresponding variation in the central value of the cross section will not be included in the systematics uncertainties calculus.

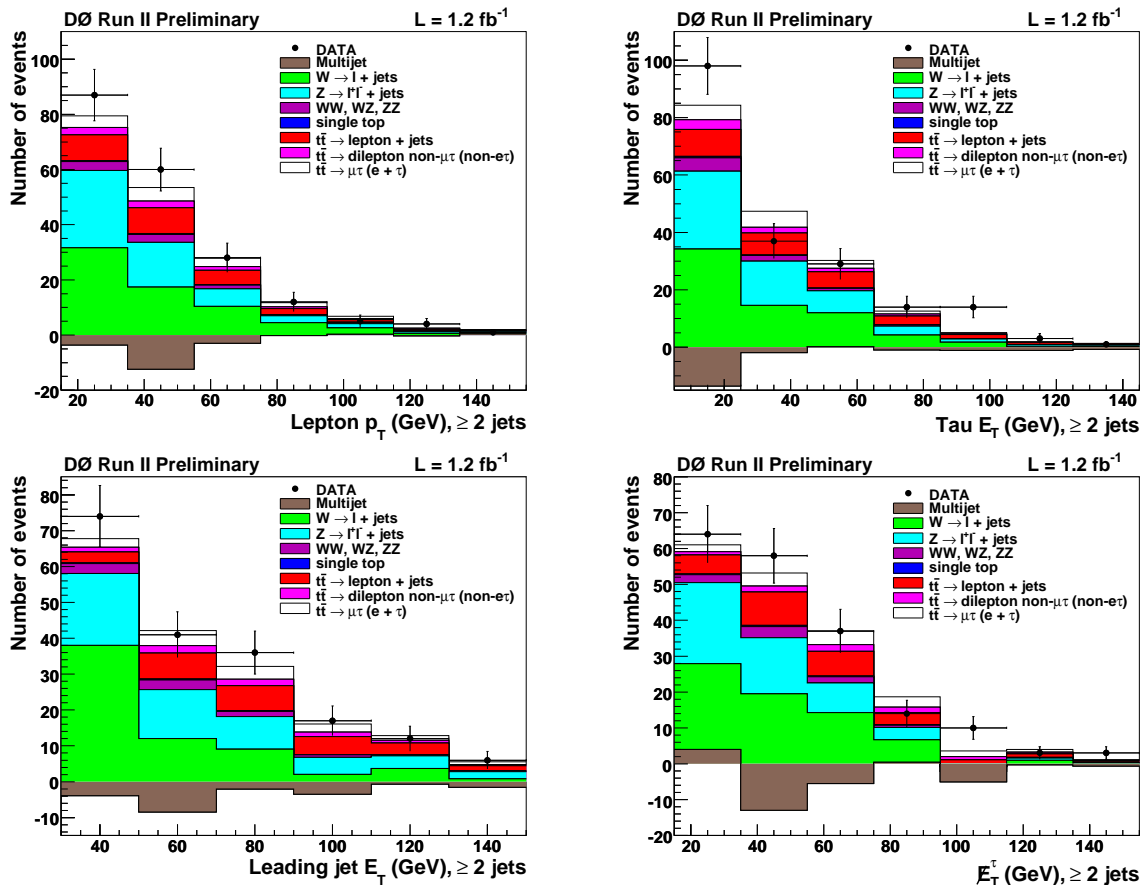


FIG. 1: Distributions of lepton  $p_T$  (top left); tau  $p_T$  (top right); leading jet  $p_T$  (bottom left) and  $\cancel{E}_T$  (bottom right) in  $e\tau + \mu\tau$  channel before  $b$ -tagging requirement. Expected contribution from  $t\bar{t}$  events is normalized using the SM cross section of  $\sigma(t\bar{t})=7.91$  pb.

Systematics uncertainties originate from various sources. Experimental uncertainties arise from the trigger simulation, from the jet energy calibration, resolution, reconstruction efficiency, from  $b$ -tagging, lepton identification, tau reconstruction, tau fake rate and primary vertex (PV) identification. Uncertainties on the MC normalization include normalization and flavor composition uncertainties. The cross sections of the various SM processes suffer from theoretical uncertainties (normalization and flavor composition). The resulting variations in the central value of the cross section are presented in Table IV. The dominant systematic uncertainty is the background/MC statistics. It is an uncorrelated combination of the statistical uncertainty on the Monte-Carlo samples and same-sign data contributions to the background.

## VIII. RESULTS AND CONCLUSIONS

The measurement of the production cross section of top quark pairs in the  $\ell + \tau$  channel ( $\ell = e, \mu$ ) in Run IIb has been performed. The results for a top mass of 170 GeV are:

$$\begin{aligned} \mu + \tau : \sigma(t\bar{t}) &= 7.84^{+2.66}_{-2.28}(\text{stat})^{+1.46}_{-1.44}(\text{syst}) \pm 0.48(\text{lumi}) \text{ pb}, \\ e + \tau : \sigma(t\bar{t}) &= 5.05^{+2.95}_{-2.51}(\text{stat})^{+2.25}_{-2.23}(\text{syst}) \pm 0.31(\text{lumi}) \text{ pb}. \end{aligned}$$

The results for a top mass of 175 GeV are:

$$\begin{aligned}\mu\tau : \sigma(t\bar{t}) &= 7.56^{+2.56}_{-2.20}(\text{stat})^{+1.57}_{-1.49}(\text{syst}) \pm 0.46(\text{lumi}) \text{ pb} \\ e\tau : \sigma(t\bar{t}) &= 4.72^{+2.76}_{-2.34}(\text{stat})^{+2.13}_{-2.09}(\text{syst}) \pm 0.29(\text{lumi}) \text{ pb}\end{aligned}$$

The combined cross section for  $e\tau$  and the  $\mu\tau$  channels is obtained by minimizing the sum of the negative log-likelihood functions for each individual channel. All uncertainties are treated as correlated between the  $\mu\tau$  and  $e\tau$  channels except for the individual muon or electron uncertainties and the background statistics uncertainty. Assuming a top mass of 170 GeV:

$$\ell + \tau : \sigma(t\bar{t}) = 6.75^{+1.91}_{-1.70}(\text{stat})^{+1.49}_{-1.31}(\text{syst}) \pm 0.41(\text{lumi}) \text{ pb.}$$

Assuming a top mass of 175 GeV:

$$\ell + \tau : \sigma(t\bar{t}) = 6.42^{+1.82}_{-1.62}(\text{stat})^{+1.42}_{-1.25}(\text{syst}) \pm 0.39(\text{lumi}) \text{ pb}$$

The  $e\tau$  and  $\mu\tau$  combined Run IIa cross section (using about  $1 \text{ fb}^{-1}$  of data, assuming a top mass of 175 GeV) was found to be [7] :

$$\ell + \tau : \sigma(t\bar{t}) = 8.3^{+2.0}_{-1.8}(\text{stat})^{+1.4}_{-1.2}(\text{syst}) \pm 0.5(\text{lumi}) \text{ pb}$$

The combination of the Run IIa results and the Run IIb results gives:

$$\ell + \tau : \sigma(t\bar{t}) = 7.32^{+1.34}_{-1.24}(\text{stat})^{+1.20}_{-1.06}(\text{syst}) \pm 0.45(\text{lumi}) \text{ pb}$$

This is in good agreement with the other measurements from D0 [1, 3], and with the theoretical prediction of  $7.2^{+0.7}_{-0.9}$  pb from the full NLO matrix elements and the resummation of the leading and next-to-leading soft logarithms [19], for the current Tevatron average [20] of  $m_{top}=172.6 \pm 1.4$  GeV.

- 
- [1] V.M. Abazov *et al.* (D0 Collaboration), Phys. Rev. D **76**, 052006 (2007).  
[2] D. Acosta *et al.* (CDF Collaboration), Phys. Rev. Lett. **93**, 142001, (2004).  
[3] V.M. Abazov *et al.* (D0 Collaboration), FERMILAB-PUB-08-064-E, arXiv:0803.2779v1 [hep-ex], sub. to Phys. Rev. L.  
[4] A. Abulencia *et al.* (CDF Collaboration), Phys. Rev. D **74**, 072006 (2006).  
[5] M. Abazov *et al.* (D0 Collaboration), Phys. Rev. D **76**, 072007 (2007).  
[6] T. Aaltonen *et al.* (CDF Collaboration), Phys. Rev. D **76**, 072009 (2007).  
[7] V.M. Abazov *et al.* (D0 Collaboration), D0 CONF-note 5416 (2007).  
[8] T. Andeen *et al.*, FERMILAB-TM-2365 (2007).  
[9] V.M. Abazov *et al.* (D0 Collaboration), Nucl. Instrum. Methods Phys. Res., Sect. A **565**, 463 (2006).  
[10] G. C. Blazey *et al.*, in *Proceedings of the Workshop: "QCD and Weak Boson Physics in Run II"*, edited by U. Baur, R. K. Ellis, and D. Zeppenfeld, FERMILAB-PUB-00-297, p47 (2000).  
[11] V.M. Abazov *et al.* (D0 Collaboration), Phys. Rev. D **71**, 072004 (2005).  
[12] T. Scanlon, FERMILAB-THESIS-2006-43.  
[13] M.L. Mangano *et al.*, JHEP **307**, 001 (2003).  
[14] T. Sjostrand, P. Eden, C. Friberg, L. Lonnblad, G. Miu, S. Mrenna and E. Norrbin, Computer Phys. Commun. **135**, 238 (2001).  
[15] A. Pukhov *et al.*, CompHEP - User's manual for version 3.3, arXiv:hep-ph/990888,  
A.S. Belyaev *et al.*, CompHEP - PYTHIA interface, arXiv:hep-ph/0101232.  
[16] S. Jadach, Z. Was, R. Decker, and J. H. Kuhn, Computer Phys. Commun. **76**, 361 (1993).  
[17] D. J. Lange, Nucl. Instrum. Methods Phys. Res., Sect. A **462**, 152 (2001).  
[18] R. Hamberg, W. L. van Neerven, and T. Matsuura, Nucl. Phys. **B359**, 343 (1991) [Erratum-ibid. **B644**, 403 (2002)].  
[19] N. Kidonakis and R. Vogt, Phys. Rev. D **68**, 114014 (2003).  
[20] The Tevatron Electroweak Working Group, FERMILAB-TM-2403-E.

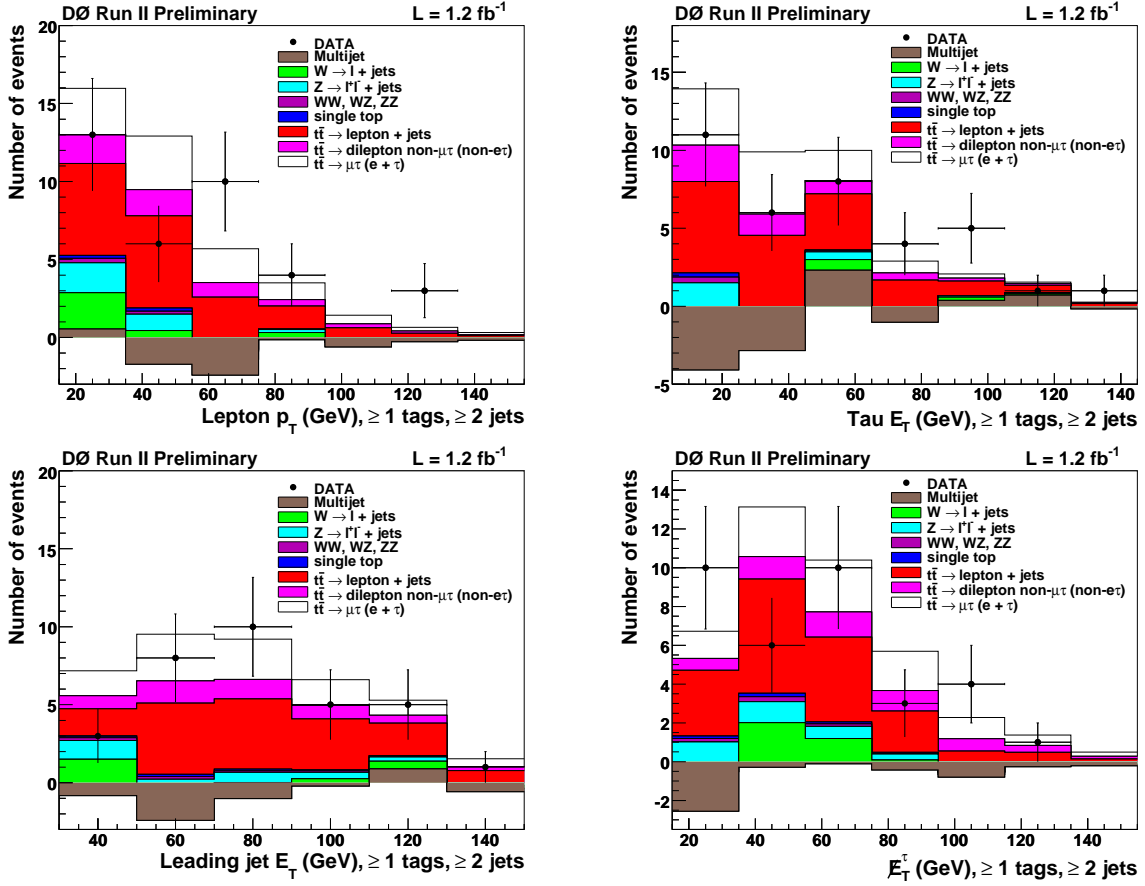


FIG. 2: Distributions of lepton  $p_T$  (top left); tau  $p_T$  (top right); leading jet  $p_T$  (bottom left) and  $E_T^{\tau}$  (bottom right) in  $e\tau+\mu\tau$  channel after  $b$ -tagging requirement. Expected contribution from  $t\bar{t}$  events is normalized using the SM cross section of  $\sigma(t\bar{t})=7.91$  pb.

TABLE IV: Systematics for the measurement of  $\sigma(t\bar{t})$ .

	$\mu\tau$	$e\tau$
	$\Delta\sigma$ (pb)	$\Delta\sigma$ (pb)
Jet energy calibration	+0.16 -0.23	+0.20 -0.17
PV identification	+0.08 -0.08	+0.06 -0.06
Muon identification	+0.21 -0.21	-
Electron identification	-	+0.38 -0.34
Tau identification	+0.30 -0.28	+0.17 -0.16
Trigger	+0.37 -0.34	+0.16 -0.06
Jet-tau fake rate	+0.31 -0.30	+0.27 -0.25
Opposite charge	+0.19 -0.19	+0.13 -0.1
$b$ -tagging	+0.51 -0.44	+0.37 -0.33
MC normalization	+0.31 -0.31	+0.30 -0.30
Background/MC statistics	+1.14 -1.14	+2.12 -2.12
Luminosity profile	+0.19 -0.19	+0.13 -0.13
Total	+1.46 -1.44	+2.25 -2.23